

## Capacitance pressure sensor based on GaN high-electron-mobility transistor-on-Si membrane

B. S. Kang, J. Kim, S. Jang, and F. Ren

*Department of Chemical Engineering, University of Florida, Gainesville, Florida 32611*

J. W. Johnson, R. J. Therrien, P. Rajagopal, J. C. Roberts, E. L. Piner, and K. J. Linthicum

*Nitronex Corporation, Raleigh, North Carolina 27606*

S. N. G. Chu

*Multiplex, Inc., South Plainfield, New Jersey 07080*

K. Baik, B. P. Gila, C. R. Abernathy, and S. J. Pearton<sup>a)</sup>

*Department of Materials Science and Engineering, University of Florida, Gainesville, Florida 32611*

(Received 19 November 2005; accepted 15 May 2005; published online 13 June 2005)

The changes in the capacitance of the channel of an AlGaIn/GaN high-electron-mobility transistor (HEMT) membrane structure fabricated on a Si substrate were measured during the application of both tensile and compressive strain through changes in the ambient pressure. The capacitance of the channel displays a change of  $7.19 \pm 0.45 \times 10^{-3}$  pF/ $\mu\text{m}$  as a function of the radius of the membrane at a fixed pressure of +9.5 bar and exhibits a linear characteristic response between  $-0.5$  and  $+1$  bar with a sensitivity of 0.86 pF/bar for a 600  $\mu\text{m}$  radius membrane. The hysteresis was 0.4% in the linear range. These AlGaIn/GaN HEMT membrane-based sensors appear to be promising for both room-temperature and elevated-temperature pressure-sensing applications. © 2005 American Institute of Physics. [DOI: 10.1063/1.1952568]

There are a number of applications in the automotive, aerospace, and industrial fields for robust miniaturized pressure sensors. A number of different semiconductor systems have been used to make piezoresistive or capacitive sensors, including Si,<sup>1</sup> SiC,<sup>2-4</sup> and diamond.<sup>5</sup> The wide-bandgap semiconductors are capable of operating at much higher temperatures than Si, with SiC-based piezoresistive sensors demonstrated up to temperatures of 600 °C.<sup>2-4</sup> We have previously demonstrated that AlGaIn/GaN high-electron-mobility transistors (HEMTs) show a strong dependence of the conductance of the channel when a membrane structure fabricated on a Si substrate was measured during changes in the ambient pressure.<sup>6-8</sup> However, one drawback of piezoresistive sensors is that contact resistance changes significantly with temperature and may mask the changes in sensor signal from actual pressure changes.<sup>4</sup> By sharp contrast, capacitive pressure sensors are less sensitive to variations in contact resistance and in addition, sensors based on AlGaIn/GaN HEMTs could be readily integrated with off-chip wireless communication chips that eliminate additional wiring capacitance. AlGaIn/GaN HEMTs have demonstrated extremely promising results for use in broadband power amplifiers in wireless base station applications.<sup>9-14</sup> The high electron sheet carrier concentration of nitride HEMTs is induced by piezoelectric polarization of the strained AlGaIn layer and spontaneous polarization,<sup>15-17</sup> suggesting that nitride HEMTs are excellent candidates for robust pressure sensing.

In this letter, we demonstrate that circular AlGaIn/GaN diaphragms fabricated with radii 200–600  $\mu\text{m}$  on Si substrates show linear changes in capacitance over a range of applied pressure and that the sign of the capacitance change is reversed when vacuum is applied to the diaphragm.

The sensors used to monitor the differential pressure are made of a circular membrane of an AlGaIn/GaN HEMT on a Si substrate. The membrane is fabricated by etching a circular hole in the substrate, as is shown schematically in Fig. 1 (top). A scanning electron microscope (SEM) cross-sectional view of an actual device is shown at the bottom of Fig. 1. A deflection of the membrane away from the substrate due to differential pressure on the two sides of the membrane pro-

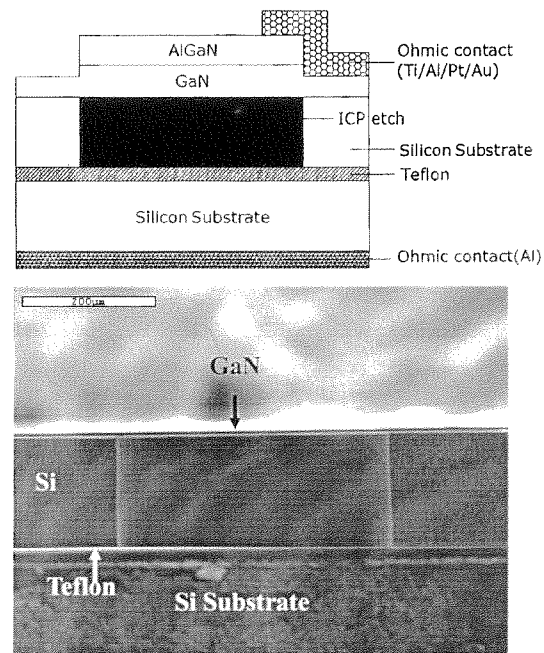


FIG. 1. Schematic diagram of device structure (top) and SEM micrograph of AlGaIn/GaN circular membrane on a Si substrate fabricated by etching a circular hole in the substrate (bottom). The latter picture is taken prior to fabrication of the HEMT device.

<sup>a)</sup>Electronic mail: speart@mse.ufl.edu

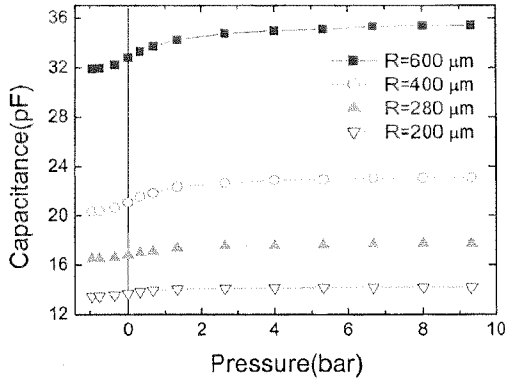
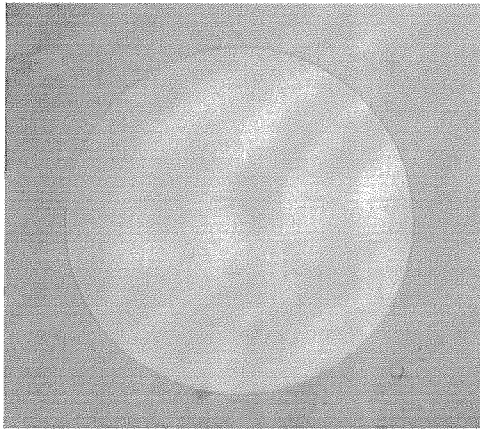


FIG. 2. Top view of HEMT capacitance pressure sensor (top) and capacitance as a function of pressure for different diaphragm radii (bottom).

duces a tensile strain in the membrane. This leads to a change in the piezo-induced two-dimensional electron gas (2DEG) density at the AlGaIn/GaN interface. This in turn affects the capacitance of the HEMT diaphragm. The carrier density is therefore directly correlated with the tensile strain in the membrane and hence with the differential pressure. We have previously calculated the radial strain  $\epsilon_r$  in the membrane as a function of the differential pressure  $P_1 - P_0$ ,<sup>7</sup> by employing a modified Stoney analysis.<sup>18,19</sup> The individual devices usually are electrically isolated by etching into a mesa structure. This breaks the continuity of the top thin layer and partially relaxes the bending strain in the AlGaIn layer. Let  $r$  be the fraction of remaining bending strain in the AlGaIn layer, then  $r < 1$  for the mesa structure. In this case,<sup>19,20</sup>  $n_s = (1/e) \{-|\Delta P_{SP}| + |\Delta \epsilon_{\text{GaIn}}| r_{\text{GaIn}} - |e_{\text{eff}} \Delta \epsilon_{\text{AlGaIn}}| \times r_{\text{AlGaIn}} + [|e_{\text{eff}}(\text{GaN})| - |e_{\text{eff}}(\text{AlGaIn})| r] \epsilon_a\}$ , where  $n_s$  is the sheet charge in the 2DEG,  $e$  is the electronic charge,  $P_{SP}$  is the spontaneous polarization,  $r_{\text{GaIn}}$  is the fraction of the final misfit strain in GaN,  $\epsilon_{\text{GaIn}}$  the misfit strain in the GaN,  $e_{\text{eff}}$  the effective piezoelectric coefficients ( $=e_{31} - e_{33} C_{13}/C_{33}$ ),  $r_{\text{AlGaIn}}$  is the fraction of unrelaxed mismatch of  $\text{Al}_x\text{Ga}_{1-x}\text{N}$  layer in the unbended state,  $r$  is the radius of curvature of the membrane, and the strain  $\epsilon_a$  in the top film for a small deflection  $d$  of the free end is approximately given by  $\epsilon_a = t_{\text{sub}} d / L^2$ . The capacitance of the 2DEG channel is then given by  $C = \{e \epsilon_0 \epsilon n / 2 (V_{bi} + V)\}^{0.5}$ , so that a change in  $n$  leads to a change in  $C$ . By monitoring the conductance of the HEMT on membrane, the pressure difference  $P_1 - P_0$  can be obtained.

The HEMTs were grown by metalorganic chemical vapor deposition on 100 mm (111) Si substrates at Nitronex

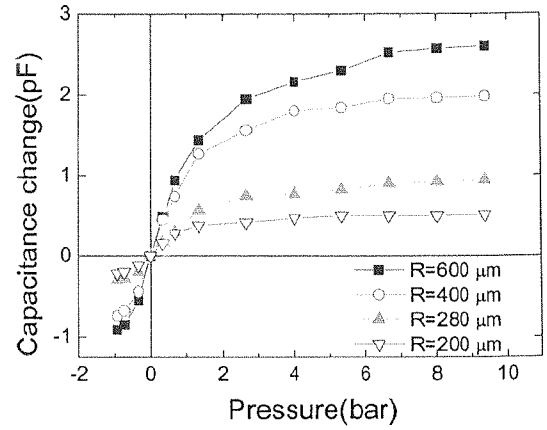


FIG. 3. AlGaIn/GaN HEMT membrane capacitance change as a function of pressure for different diaphragm radii.

Corporation. The structures consisted of an (Al, Ga)N-based transition layer, a  $\sim 0.8 \mu\text{m}$  undoped GaN buffer, and a  $300 \text{ \AA}$  undoped AlGaIn barrier layer. Mesa isolation was performed with an inductively coupled plasma (ICP) etching with  $\text{Cl}_2/\text{Ar}$ -based discharges at  $-90 \text{ V}$  dc self-bias, ICP power of  $300 \text{ W}$  at  $2 \text{ MHz}$  and a process pressure of  $5 \text{ mTorr}$ . A Ti/Al/Pt/Au-based interdigitated finger pattern separated by  $4 \mu\text{m}$  was formed with e-beam deposition and standard lift-off. The fingers were annealed at  $850 \text{ }^\circ\text{C}$ ,  $45 \text{ s}$  under flowing  $\text{N}_2$ . Plated Au was subsequently deposited on the ohmic metal pads for wire bonding on the samples. Ohmic contact for the silicon used  $1000 \text{ \AA}$  Al deposited by using sputter and annealed in nitrogen at  $300 \text{ }^\circ\text{C}$ . Via holes were fabricated from the backside of the Si substrate and stopping on the GaN layer using ICP etching with  $\text{SF}_6/\text{Ar}$ . The etch selectivity is more than  $1000:1$ .  $2000 \text{ \AA}$  of AuSn was deposited on the backside of the sample and a glass slice. The Teflon<sup>®</sup> bonding spin coating on the silicon wafer employed liquid Teflon (CYTOP CTL-809M, from Bellex International Corp.) at  $5000 \text{ rpm}$  to a thickness of  $\sim 5000 \text{ \AA}$  and then flip-chip bonding (RD automation flip-chip bonder) the fabricated device using a mechanical force of  $1000 \text{ g}$  between the upper and lower chucks for  $10 \text{ min}$  and finally baking for  $1 \text{ h}$  at  $200 \text{ }^\circ\text{C}$  to solidify the Teflon to seal off the via holes. Figure 2 (top) shows a top view of a completed HEMT capacitive pressure sensor.

The capacitances of the HEMT diaphragm structures were obtained from measurements on an Agilent 4156C parameter analyzer while the device was measured at  $25 \text{ }^\circ\text{C}$  under either vacuum ( $-1 \text{ bar}$ ) or pressure ( $+9.5 \text{ bar}$ ) conditions.

Figure 2 (bottom) shows the capacitance from the membrane HEMT structure as a function of the ambient pressure, for different membrane radii. This capacitance increases with increasing pressure and decreases under vacuum conditions, due to corresponding changes in the carrier density in the 2DEG. The metal contact area in the membrane is  $100 \times 100 \mu\text{m}^2$ , while the diameter of the membrane is  $1.2 \text{ mm}$ , and thus the metal contact area compared to the size of the membrane is negligible. The change of the capacitance due to the external pressure from the metal contacts can be ignored since the change of the distance between two metal contact is so small. With a simple calculation of the relative contributions, the maximum bending is in the center of the membrane and assumed to be  $1 \mu\text{m}$  (the bending of our cantilever is

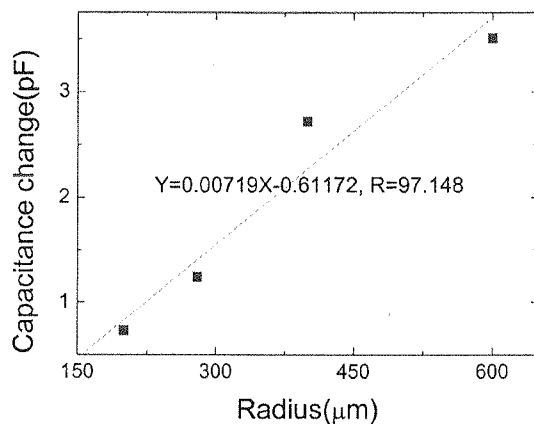


FIG. 4. Capacitance change as a function of radius of the AlGaIn/GaN HEMT membrane over the pressure range from  $-1$  to  $+9.5$  bar.

less than 1/10 of this amount) the capacitance change due to this displacement will be 0.3% of the total capacitance change. Our data showed much larger changes of capacitance from external pressure changes, therefore, it has to come from carrier density change not from displacement of the membrane. The resulting capacitance change derived from this data is shown as a function of pressure in Fig. 3. In the case of applied positive pressure, which corresponds to compressive strain induced in the HEMT layers, the capacitance increases in a linear fashion over the range between 0 and  $+1$  bar with a sensitivity of  $0.86$  pF/bar for a  $600$   $\mu\text{m}$  radius membrane. For the case of applied negative pressure (vacuum), the conductivity shows a sensitivity of the same value within experimental error to a vacuum of  $-0.5$  bar. Within the linear range, the devices exhibited a hysteresis of  $<0.4\%$ . Outside these pressure limits, the sensor has reduced sensitivity due to the device geometry. The sensitivity could be increased by having a shallower via depth, obtained by thinning the Si substrate. These trends are similar to those observed with actual bending of HEMT samples on a cantilever beam to produce tensile or compressive strain,<sup>6</sup> but exhibit much larger sensitivities to the induced tensile or compressive strain. This is due to the absence of the thick sapphire substrate that is present in the cantilever structures,<sup>6</sup> as we also reported for the piezoconductance membrane sensors previously.<sup>7</sup>

Figure 4 shows the capacitance change as a function of radius of the AlGaIn/GaN HEMT membrane at a fixed pressure of  $+9.5$  bar. The capacitance of the channel displays a change of  $7.19 \pm 0.45 \times 10^{-3}$  pF/ $\mu\text{m}$ . The sensor characteristics measured at this same pressure on several different days showed a maximum capacitance variation of  $0.07$  pF, corresponding to a sensing repeatability of  $\sim 0.15$  bar. The high-temperature characteristics still need to be established, but in this case will be limited by the thermal stability of the ohmic contacts. Recent reports have shown that some contact met-

allizations on GaN HEMTs are stable for extended periods at  $500$   $^{\circ}\text{C}$ .<sup>21</sup>

In summary, a AlGaIn/GaN HEMT membrane on Si shows large changes in capacitance as a result of changes in ambient pressure. This approach is less sensitive to contact resistance variations with temperature than the previous conductance sensors. The sensors can also be readily integrated with conventional HEMTs or Si circuitry to provide off-chip wireless transmission of pressure data.

The work at UF is partially supported by AFOSR (F49620-02-1-0366, G. Witt, and F49620-03-1-0370), NSF (CTS-0301178, monitored by Dr. M. Burka and Dr. D. Senich), by NASA Kennedy Space Center Grant NAG 10-316 monitored by Mr. Daniel E. Fitch, ONR (N00014-98-1-02-04, H. B. Dietrich), and NSF DMR 0400416 (L. Hess).

- <sup>1</sup>W. H. Ko and Q. Wang, *Sens. Actuators, A* **75**, 242 (1999).
- <sup>2</sup>A. A. Ned, R. S. Okojic, and A. D. Kurtz, *Proc. High Temp. Electronics Conf.* (IEEE, Piscataway, NJ, 1998), Vol. 14–18, pp. 257–260.
- <sup>3</sup>C. H. Wu, S. Stefanescu, H. I. Kuo, C. A. Zorman, and M. Mehregany, *Proc. Int. Conf. Solid-State Sensors and Actuators*, Copenhagen, Denmark, July 1997, pp. 514–517.
- <sup>4</sup>D. J. Young, J. Du, C. A. Zorman, and W. H. Ko, *IEEE Sens. J.* **4**, 464 (2004).
- <sup>5</sup>J. L. Davidson, D. R. Wur, W. P. Kang, D. Kinser, and D. V. Kerns, *Proc. Symp. Microstructures and Microfabricated Systems* (Electrochem. Soc., Pennington, NJ, 1994), Vol 94–14, pp. 30–37.
- <sup>6</sup>B. S. Kang, S. Kim, J. Kim, F. Ren, K. Baik, S. J. Pearton, B. Gila, C. R. Abernathy, C. Pan, G. Chen, J. I. Chyi, V. Chandrasekaran, M. Sheplak, T. Nishida, and S. N. G. Chu, *Appl. Phys. Lett.* **83**, 4845 (2003).
- <sup>7</sup>B. S. Kang, S. Kim, F. Ren, J. W. Johnson, R. Therrien, P. Rajagopal, J. Roberts, E. Piner, K. J. Linthicum, S. N. G. Chu, K. Baik, B. P. Gila, C. R. Abernathy, and S. J. Pearton, *Appl. Phys. Lett.* **85**, 2962 (2004).
- <sup>8</sup>S. J. Pearton, B. S. Kang, S. Kim, F. Ren, B. P. Gila, C. R. Abernathy, J. Lin, and S. N. G. Chu, *J. Phys.: Condens. Matter* **16**, R961 (2004).
- <sup>9</sup>A. Tarakji, X. Hu, A. Koudymov, G. Simin, J. Yang, M. A. Khan, M. S. Shur, and R. Gaska, *Solid-State Electron.* **46**, 1211 (2002).
- <sup>10</sup>A. P. Zhang, L. B. Rowland, E. B. Kaminsky, V. Tilak, J. C. Grande, J. Teetsov, A. Vertiatchikh, and L. F. Eastman, *J. Electron. Mater.* **32**, 388 (2003).
- <sup>11</sup>S. J. Pearton, J. C. Zolper, R. J. Shul, and F. Ren, *J. Appl. Phys.* **86**, 1 (1999).
- <sup>12</sup>A. Koudymov, X. Hu, K. Simin, G. Simin, M. Ali, J. Yang, and M. A. Khan, *IEEE Electron Device Lett.* **23**, 449 (2002).
- <sup>13</sup>A. P. Zhang, G. T. Dang, F. Ren, H. Cho, K. P. Lee, S. J. Pearton, J.-I. Chi, T. E. Nee, C. M. Lee, and C. C. Chuo, *IEEE Trans. Electron Devices* **48**, 407 (2001).
- <sup>14</sup>M. S. Shur, *Solid-State Electron.* **42**, 2131 (1998).
- <sup>15</sup>O. Ambacher, B. Foutz, J. Smart, J. R. Shealy, N. G. Weimann, K. Chu, M. Murphy, W. J. Schaff, L. Wittmer, L. E. Eastman, R. Dimitrov, A. Mitchell, and M. Stutzmann, *J. Appl. Phys.* **87**, 334 (2000).
- <sup>16</sup>O. Ambacher, J. Smart, J. R. Shealy, N. G. Weimann, K. Chu, M. Murphy, W. J. Schaff, L. E. Eastman, R. Dimitrov, L. Wittmer, M. Stutzmann, W. Rieger, and J. Hilsenbeck, *J. Appl. Phys.* **85**, 3222 (1999).
- <sup>17</sup>P. M. Asbeck, E. T. Yu, S. S. Lau, G. J. Sullivan, J. Van Hove, and J. M. Redwing, *Electron. Lett.* **33**, 1230 (1997).
- <sup>18</sup>G. G. Stoney, *Proc. R. Soc. London* **82**, 172 (1909).
- <sup>19</sup>S. N. G. Chu, *J. Electrochem. Soc.* **145**, 3621 (1998).
- <sup>20</sup>S. N. N. Chu, F. Ren, S. J. Pearton, B. S. Kang, S. Kim, B. P. Gila, C. R. Abernathy, J.-I. Chyi, W. J. Johnson, and J. Lin, presented at TMS Annual Meeting, San Francisco, February 2005.
- <sup>21</sup>D. Selvanathan, F. M. Mohammed, A. Tesfayesus, and I. Adesida, *J. Vac. Sci. Technol. B* **22**, 2409 (2004).